



# Magnetic Actuation of Drops and Liquid Marbles Using a Deformable Paramagnetic Liquid Substrate

Jacopo Vialletto, Masayuki Hayakawa, Nikita Kavokine, Masahiro Takinoue, Subramanyan Namboodiri Varanakkottu, Sergii Rudiuk, Manos Anyfantakis, Mathieu Morel, and Damien Baigl\*

**Abstract:** The magnetic actuation of deposited drops has mainly relied on volume forces exerted on the liquid to be transported, which is poorly efficient with conventional diamagnetic liquids such as water and oil, unless magneto-sensitive particles are added. Herein, we describe a new and additive-free way to magnetically control the motion of discrete liquid entities. Our strategy consists of using a paramagnetic liquid as a deformable substrate to direct, using a magnet, the motion of various floating liquid entities, ranging from naked drops to liquid marbles. A broad variety of liquids, including diamagnetic (water, oil) and nonmagnetic ones, can be efficiently transported using the moderate magnetic field (ca. 50 mT) produced by a small permanent magnet. Complex trajectories can be achieved in a reliable manner and multiplexing potential is demonstrated through on-demand drop fusion. Our paramagnetofluidic method advantageously works without any complex equipment or electric power, in phase with the necessary development of robust and low-cost analytical and diagnostic fluidic devices.

Controlling the motion of drops on surfaces is the cornerstone of a broad range of scientific and technological operations.<sup>[1,2]</sup> In the large majority of cases, the drop motion is induced by an interfacial energy gradient at a solid/liquid interface (wettability gradient) and/or at a free interface (Marangoni stress).<sup>[3]</sup> This has resulted in a plethora of studies to elucidate the fundamental mechanisms that convert such gradients into drop motion<sup>[4]</sup> as well as to develop strategies to manipulate drops under the control of

various external signals, such as thermal,<sup>[5]</sup> electrical<sup>[2,6,7]</sup> and optical<sup>[8–13]</sup> stimuli. Most of these approaches necessitate the implementation of rather complex components, such as electrodes or optical elements, or the development of systems that are intrinsically responsive to the desired stimulus, such as photo- or thermosensitive substrates.<sup>[8,9]</sup> This has led to the emergence of a broad variety of powerful drop actuation strategies that work in a laboratory environment, that is, require specific equipment and well-controlled conditions (for example, protection from ambient light or precise control of temperature and surface tension). However, broadly applicable strategies for robust and cost-effective manipulation of discrete liquid entities have yet to be identified. Apart from thermal, optical, and electrical stimulation, magnetic field-induced drop actuation could be the basis to achieve such a goal.<sup>[14,15]</sup> In particular, permanent magnets are available in a variety of sizes and shapes at affordable prices and can be easily handled without any specific environmental requirement. However, although drops composed of strongly responsive fluids, such as paramagnetic liquids<sup>[16,17]</sup> or ferrofluids,<sup>[18–20]</sup> are commonly actuated by magnets, the majority of conventional drops are made of diamagnetic liquids (for example, water and oil) and cannot be efficiently manipulated unless a strong magnetic field is applied. To our knowledge, the only strategy for moving discrete diamagnetic liquid entities in air using moderate magnetic fields has consisted in using magnetosensitive particles, dispersed inside the liquid<sup>[21]</sup> or coating the liquid to form liquid marbles.<sup>[14,22–25]</sup> Using magnetic particles inside or outside the liquid increases

[\*] J. Vialletto, N. Kavokine, Dr. S. N. Varanakkottu, Dr. S. Rudiuk, Dr. M. Anyfantakis, Dr. M. Morel, Prof. Dr. D. Baigl  
PASTEUR, Department of chemistry, École Normale Supérieure, UPMC Univ. Paris 06, CNRS, PSL Research University  
75005 Paris (France),  
and  
Sorbonne Universités, UPMC Univ. Paris 06, École Normale Supérieure, CNRS, PASTEUR  
75005 Paris (France)  
E-mail: damien.baigl@ens.fr  
Homepage: <http://www.baigllab.com/>  
N. Kavokine  
Laboratoire de Physique Statistique, Ecole Normale Supérieure, PSL Research University  
24 rue Lhomond, 75005 Paris (France)  
Dr. M. Hayakawa, Prof. M. Takinoue  
Department of Computer Science, Tokyo Institute of Technology  
Kanagawa 226-8502 (Japan)

Dr. S. N. Varanakkottu  
Current address: School of Nano Science and Technology Calicut, National Institute of Technology  
Kozhikode (India)  
Dr. M. Anyfantakis  
Current address: University of Luxembourg, Physics & Materials Science Research Unit  
162a Avenue de la Faiencerie, Luxembourg L-1511 (Luxembourg)  
Dr. M. Hayakawa  
Current address: RIKEN Quantitative Biology Center, Kobe 650-0047 (Japan)

Supporting information and the ORCID identification number(s) for the author(s) of this article can be found under:  
<https://doi.org/10.1002/anie.201710668>.

© 2017 The Authors. Published by Wiley-VCH Verlag GmbH & Co. KGaA. This is an open access article under the terms of the Creative Commons Attribution-NonCommercial License, which permits use, distribution and reproduction in any medium, provided the original work is properly cited and is not used for commercial purposes.

sample cost, reduces applicability, and poses the problem of sample contamination. Moreover, although liquid marbles allow efficient liquid transport,<sup>[26,27]</sup> they remain, unlike their drop counterparts, difficult to merge and split apart for digital fluidic operations.<sup>[2]</sup> Herein, we propose a new way to move and merge any kind of discrete liquid entity, including diamagnetic and nonmagnetic ones, using external small permanent magnets. Our method does not require the use of any magnetosensitive particles, nor has it any specific restrictions in terms of environmental conditions. It consists in using a paramagnetic liquid as a substrate and exploits the deformation induced by an approaching magnet as the driving force for a floating entity. To our knowledge, although the magnetic field-induced deformation of a paramagnetic liquid is a well-known phenomenon that has been used in various scientific fields,<sup>[28,29]</sup> it has never been exploited to transport guest liquid entities. We characterized the deformation induced by small permanent magnets and analyzed the resulting motion of different floating entities, including oil drops and water-based liquid marbles of various compositions. We also experimentally and theoretically quantified the marked contribution of the substrate deformation to the motion of a floating object under magnetic stimulation. We finally used mobile magnets to perform various operations such as long-term transport along complex trajectories and magnetically controlled drop fusion.

Our experimental set-up consisted of a Petri dish containing a paramagnetic  $\text{HoCl}_3$  solution used as a deformable substrate. The liquid thickness (5.2 mm) was fixed at a value larger than the capillary length of the system (ca. 2.7 mm). A portable, permanent NdFeB magnet was released from a fixed position far from the substrate surface to follow a free fall trajectory and reach a second fixed position close to the substrate surface (12.7 mm), resulting in motion of floating objects deposited on the substrate. We first used a 2  $\mu\text{L}$  liquid marble (LM), made of hydrophobically modified silica nanoparticles surrounding a water core,<sup>[27]</sup> as the entity to be transported (Figure 1A). With the magnet maintained in position 1, no marble motion was detected. Switching the magnet from position 1 to 2 led to an immediate and radial motion of the marble away from the magnet axis (Figure 1B and the Supporting Information, Movie S1). To our knowl-

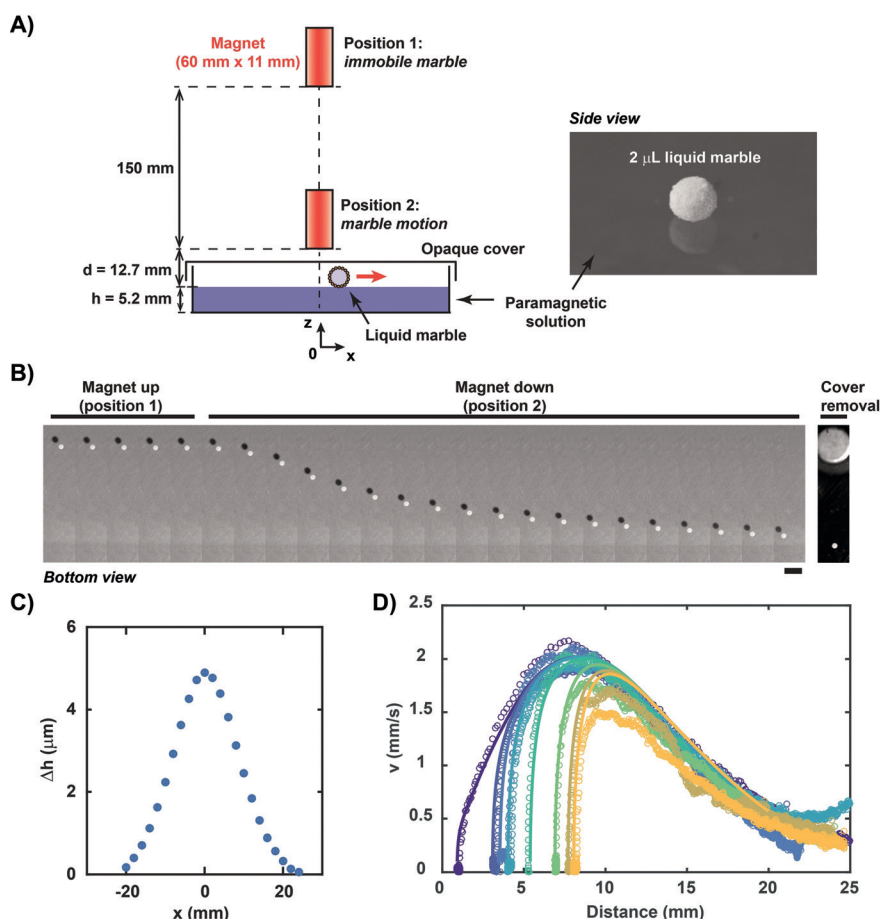


**Figure 1.** Magnetic actuation of a water liquid marble on a paramagnetic liquid substrate. A) Experimental set-up with a 2  $\mu\text{L}$  water liquid marble (diameter 1.6 mm) floating on a paramagnetic solution ( $[\text{HoCl}_3] = 100 \text{ mM}$ ) in a closed Petri dish. The free-fall switch of a permanent magnet from position 1 (far from the substrate surface) to position 2 (close to the substrate surface) induces marble motion. B) Kymograph of the marble (bottom view) upon switching the magnet from position 1 (up) to position 2 (down). The white and black disks are the marble and its shadow, respectively. Frames are separated by 2 s. Scale bar = 5 mm. The last image on the right indicates the position of the magnet that can be seen once the cover has been removed. The corresponding video is provided as Movie S1. C) Radial elevation of the substrate surface,  $\Delta h$ , when the magnet is switched from position 1 to position 2. Error bars are smaller than the symbol size. D) Speed of the liquid marble as a function of the distance to the central axis of the magnet. Each curve corresponds to a different initial position. Symbols are experimental data and solid lines are theoretical curves calculated using the experimental measurements of both magnetic field profile and surface deformation and the same value of  $C$  for all curves (Supporting Information, Section S1).

edge, this is the first reported magnetically induced motion of a liquid marble that does not contain any ferromagnetic or paramagnetic component (in the coating particles or in the inner core). A key component of this motion is the deformation of the substrate resulting from the applied magnetic field (Supporting Information, Figure S1). When the magnet was switched from position 1 to position 2, the surface was elevated toward the magnet forming a stationary radially symmetric bump with a maximum height of about 5  $\mu\text{m}$  and a radial extent of about 20 mm (Figure 1C), thus creating a slope onto which the marble could slide.<sup>[27]</sup> Regardless of the initial distance between the LM and the magnet axis, the LM first rapidly accelerated up to a maximal speed  $v_{\text{max}} \approx 2 \text{ mm s}^{-1}$  and then slowly decelerated (Fig-

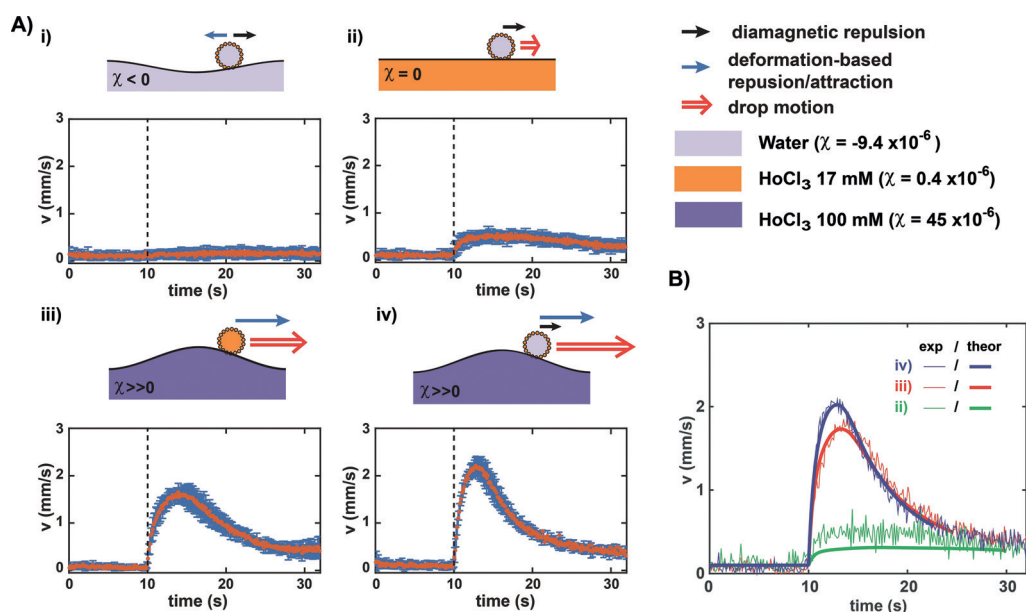


**Figure 2.** The motion is mainly driven by substrate deformation. A) Scheme of the main components of marble motion and speed as a function of time for a 2  $\mu\text{L}$  liquid marble made of water (i, ii, and iv,  $\chi < 0$ ) or 17 mM  $\text{HoCl}_3$  (iii,  $\chi \approx 0$ ) on a water substrate containing different amounts of  $\text{HoCl}_3$ : 0 mM (i,  $\chi < 0$ ); 17 mM (ii,  $\chi \approx 0$ ); and 100 mM (iii and iv,  $\chi \gg 0$ , bottom). The marble motion (double red arrow) results from the combination of the diamagnetic repulsion (black arrow) and the substrate deformation-driven gravity force (blue arrow). Each graph shows the experimental speed data (mean  $\pm$  sd for 6 independent experiments) with an initial distance between the marble and the magnet axis within the range of 0–5 mm. The dashed line indicates the time at which the magnet was switched from position 1 to 2. B) Three sets of experimental data (thin lines) taken in the three configurations in which marble motion was observed (ii, iii, and iv) and corresponding theoretical curves (thick lines) calculated with the same value of  $C$  as in Figure 1, using the experimental measurements of both magnetic field profile and surface deformation (Supporting Information, Section S1).

ure 1D, symbols). This maximal speed could be increased by simply bringing the magnet closer to the substrate. For instance, decreasing the magnet-to-substrate distance in position 2 from 12.7 mm to 9.8 mm led to  $v_{\text{max}} \approx 4.8 \text{ mm s}^{-1}$  (Supporting Information, Figure S2 and Movie S2).

We hypothesized that the two main components leading to marble motion were the diamagnetic repulsion exerted on the marble and the deformation-induced gravity force, both of which induced a repulsion of the marble from the magnet axis. To quantify the relative contribution of each component, we varied the magnetic susceptibility ( $\chi$ ) of the liquid marble as well as that of the substrate (Figure 2), by using  $\text{HoCl}_3$  solutions of different concentrations (Supporting Information, Figure S3). We first used a water LM on a water substrate ( $\chi = -9.5 \pm 0.4 \times 10^{-6}$  for both the LM and the substrate). No significant motion could be detected, which was attributed to the attractive contribution of the surface deformation (depression) counteracting the diamagnetic repulsion (Figure 2A, i). The effect of the diamagnetic repulsion only on the water LM was assessed by using a 17 mM  $\text{HoCl}_3$  solution as the substrate ( $\chi = 0.4 \pm 0.1 \times 10^{-6}$ ), so that no surface deformation occurred (Figure 2A, ii). The LM then moved at a relatively low speed ( $v_{\text{max}} = 0.6 \pm 0.1 \text{ mm s}^{-1}$ ). In contrast, a much higher speed ( $v_{\text{max}} = 1.7 \pm 0.2 \text{ mm s}^{-1}$ ) was obtained when a 17 mM  $\text{HoCl}_3$  LM was used on a 100 mM  $\text{HoCl}_3$  substrate ( $\chi = 45 \pm 1.7 \times 10^{-6}$ ), that is, in the case of a motion induced by the substrate deformation only (Figure 2A, iii). When the water LM was placed on this substrate (same conditions as in Figure 1), the strongest

response to the magnet was obtained ( $v_{\text{max}} = 2.2 \pm 0.2 \text{ mm s}^{-1}$ ) as a result of the additive contributions of both the diamagnetic repulsion and the substrate deformation (Figure 2A, iv). We built an analytical model (Supporting Information, Section S1) for the LM motion including weight, buoyancy, surface tension, drag force, and magnetic repulsion exerted on the LM floating on the liquid substrate, which led to Equation (1):

$$\frac{dv}{dt} = -\frac{v_0}{\tau} (\sin\phi)^2 \partial_r h - \frac{C \sin\phi}{\tau} v(r, t) + V \frac{\chi}{1 + \chi} \frac{\partial_r B^2}{2\mu_0 m} \quad (1)$$

where  $\tau = m/2\pi\eta a$  and  $v_0 = \gamma/\eta$  and  $\chi$ ,  $v$ ,  $m$ ,  $a$ ,  $V$  and  $\phi$  are the magnetic susceptibility, velocity, mass, radius, volume, and wrapping angle of the LM, respectively (Supporting Information, Scheme S1), and  $h(r)$  is the local elevation of the substrate,  $\mu_0$  is the vacuum permeability, and  $C$  is a numerical prefactor of the drag force (on the order of  $1^{[30]}$ ).  $\phi$  was determined according to Ooi et al.<sup>[31]</sup> and found to be around  $14^\circ$ . Equation (1) was integrated numerically using the experimentally determined values for both  $h(r)$  and  $B(r)^2$ . The only unknown parameter,  $C$ , was determined by fitting the data for the water LM on a 100 mM  $\text{HoCl}_3$  substrate and was kept constant for all other conditions. The resulting calculated curves reproduced particularly well the experimental data, even in the absence of any adjustable parameter (Figure 2B), showing that the marble motion is essentially a combination of substrate deformation-induced and diamagnetic repulsions. Our model thus confirmed the experimental



observation that the main contribution to the motion of a marble floating on a paramagnetic substrate was the magnetically induced substrate deformation and not the magnetic effect on the marble itself. Our method thus constitutes a new way to efficiently transport floating objects, even diamagnetic (for example, water) or non-magnetic (for example, 17 mM  $\text{HoCl}_3$ ) ones. Our model also reproduced well the distance-dependent behaviour (Figure 1D, solid lines), emphasizing the interest of using substrate deformation to achieve a long-range actuation of remote objects.

Liquid marbles have the remarkable advantage that they can encapsulate virtually any kind of liquid,<sup>[32]</sup> making this method of transport particularly versatile. We then wanted to know whether it can be applied to conventional liquid drops without any specific coating. We thus performed the same experiment as in Figure 1 but using a 2  $\mu\text{L}$  oil drop instead of a liquid marble. Interestingly, switching the magnet from position 1 to position 2 led to immediate motion of the drop (Figure 3A and the Supporting Information, Movie S3). To our knowledge, this is the first magnetic actuation of a diamagnetic floating liquid drop, which does not rely on any magnetosensitive solid entities such as magnetic particles. To assess the contribution of the substrate deformation to the drop motion, we performed experiments on substrates of various magnetic susceptibilities. Similarly to what was observed with the liquid marble, we could not detect any significant motion when pure water was used as a substrate (Figure 3B, left), confirming the importance of the paramagnetic nature of the substrate to achieve significant drop transport. Using a nonmagnetic substrate (17 mM  $\text{HoCl}_3$ ) in which no deformation occurred (Figure 3B, middle), resulted

in drop motion at a low speed ( $v_{\text{max}} = 0.2 \pm 0.04 \text{ mm s}^{-1}$ ), which was due to the diamagnetic repulsion exerted on the drop ( $\chi = -10.3 \pm 0.3 \times 10^{-6}$ ). In contrast, the drop acquired a much higher speed ( $v_{\text{max}} = 0.7 \pm 0.1 \text{ mm s}^{-1}$ ) when a strongly paramagnetic and thus highly deformable substrate (100 mM  $\text{HoCl}_3$ ) was used (Figure 3B, right). The same trend was observed when the concentration of  $\text{HoCl}_3$  was varied in a systematic manner. Values of  $v_{\text{max}}$  increased with an increase in  $[\text{HoCl}_3]$ , that is, when  $\chi$  and therefore the substrate deformation increased (Supporting Information, Figure S4). In the same way as for the liquid marble actuation, these results showed that the magnetically induced motion of the drop on a paramagnetic substrate (Figures 3) was mainly driven by the substrate deformation, to which was added the weak contribution of the diamagnetic repulsion. The behaviour of the velocity as a function of distance to the magnet was also similar to that of liquid marbles (Supporting Information, Figure S5). Although the liquid marble and the oil drop had a similar magnetic susceptibility, the maximum speed for the drop was typically half that of the marble, which was attributed to a stronger dissipation at the liquid/liquid interface between the drop and the paramagnetic liquid substrate.

Finally, we explored how this new universal principle for magnetically induced motion of discrete liquid entities can be exploited for more complex operations of drop manipulation. First, using a mobile and portable magnet, drop motion could be maintained for extended periods of time and complex trajectories including curves (Figure 4A and the Supporting Information, Movie S4) and self-crossing points (Supporting Information, Figure S6 and Movie S5) were easily achieved with precision. Liquid marbles were also successfully transported along complex trajectories, such as “S” and “J” shapes (Supporting Information, Figure S7). To program drop fusion, we simply used a pair of mobile magnets to move two drops toward each other and therefore guide their fusion (Figure 4B and the Supporting Information, Movie S6).

In summary, we described a new mode of interfacial transport in which magnetic field-induced liquid substrate deformation was used to actuate floating objects. This is the first method that allows the magnetically controlled actuation and manipulation of discrete liquid entities in air, which does not rely on the use of magnetosensitive particles. It was demonstrated to be particularly versatile as it is compatible with both conventional drops and liquid marbles; and any liquid, including most common diamagnetic liquids such as oil and water, can

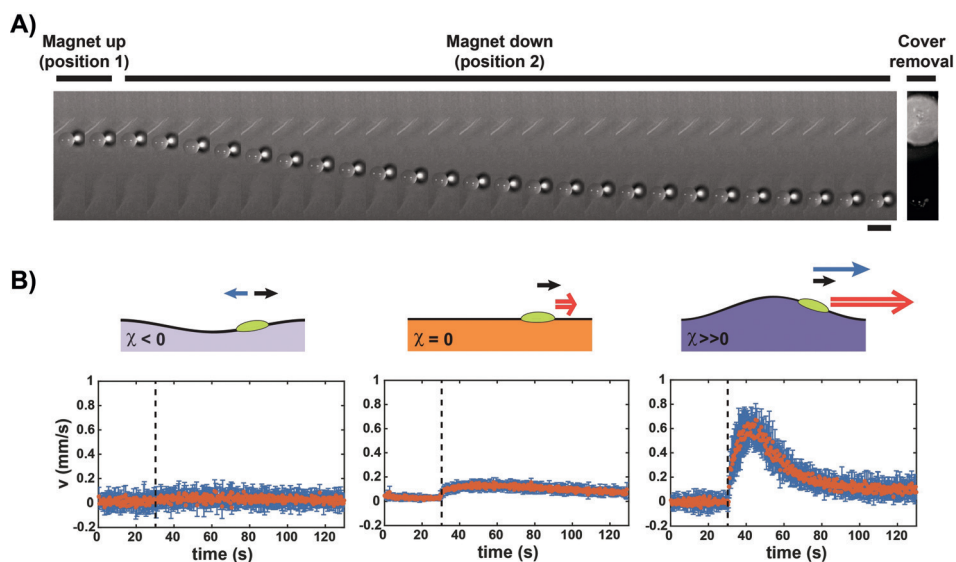


**Figure 3.** Magnetic actuation of an oil drop. A) Kymograph of the magnet-triggered motion of a 2  $\mu\text{L}$  mineral oil drop on a 100 mM  $\text{HoCl}_3$  substrate using the same experimental set-up as in Figure 1A. The bright spot surrounded by a dark ring is the shadow of the drop. Frames are separated by 1.6 s. Scale bar = 5 mm. The corresponding video is provided as Movie S3. B) Scheme (top) and speed as a function of time (bottom) of a 2  $\mu\text{L}$  mineral oil drop on a water substrate containing different amounts of  $\text{HoCl}_3$ : 0 mM (left,  $\chi < 0$ ); 17 mM (middle,  $\chi \approx 0$ ); and 100 mM (right,  $\chi \gg 0$ ). Each graph shows the experimental speed data (mean  $\pm$  sd for 10 independent experiments) with an initial distance between the drop and the magnet axis within the range of 0–5 mm. The dashed line indicates the time at which the magnet was switched from position 1 to 2.

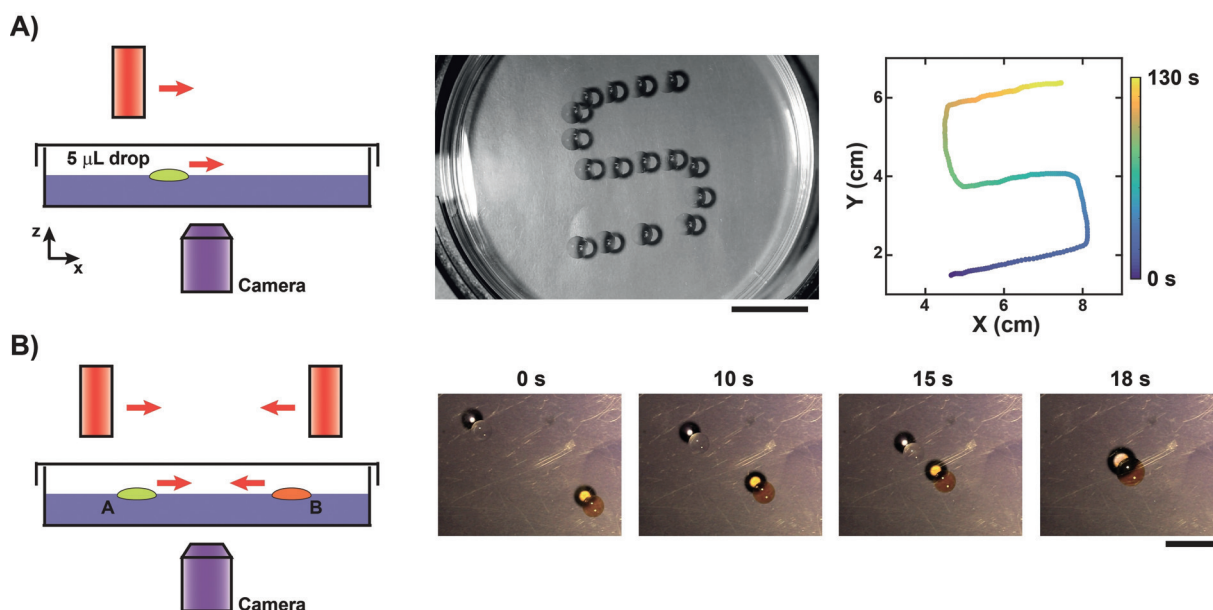


**Figure 4.** Digital magnetofluidic operations: Complex transport and fusion. A) The magnet was placed at a distance of 12 mm from the surface of a 100 mm  $\text{HoCl}_3$  substrate and manually moved to direct the motion of a 5  $\mu\text{L}$  mineral oil drop (left). Superposition of images (middle, each image separated by 8.6 s, scale bar = 2 cm) and XY positions of the drop as a function of time (right) for an imposed S-shaped trajectory. The corresponding video is provided as Movie S4. B) Two identical magnets were placed at a distance of 10 mm and moved manually to direct the motion of two 5  $\mu\text{L}$  mineral oil drops, without (drop A) and with (drop B) Sudan II dye, and induce their fusion (left). Images show the magnetically induced drop fusion (right). The scale bar = 1 cm. The corresponding video is provided as Movie S6.

be actuated. Deformation-based forces, especially capillary interactions, have been widely exploited to assemble or organize objects at interfaces,<sup>[33]</sup> but deformation-based fluidic transport<sup>[27]</sup> has been a much more rarely explored principle.<sup>[34]</sup> From a fundamental point of view, we showed that the contribution of the substrate deformation, even within a range of only a few microns, largely dominated that of the magnetic force exerted on the transported object. This made it possible to actuate the system with cost-effective permanent magnets, paving the way for a new generation of microfluidic devices powered by miniature magnets and which are able to work without complex elements such as pumps, valves, or electrodes. This electric power-free principle can also contribute to expanding the possibilities of low-cost microfluidics and diagnostics,<sup>[35,36]</sup> making solutions developed in laboratories more broadly available to people and societies.

## Acknowledgements

This work was supported by the European Research Council (ERC) [European Community's Seventh Framework Programme (FP7/2007-2013/ERC Grant Agreement No. 258782)], the Mairie de Paris [Emergence(s) 2012], the Institut de France (Subvention Scientifique Del Duca), the European Commission (FP7-PEOPLE-2013-IEF/ Project 624806 "DIOPTRA"), and the Labex IPGG (ANR-10-LABX-31). D.B. proposed the idea, conceived and supervised the entire project; S.R. and N.K. optimized the liquid marble formulation; S.N.V., M.H., and J.V. built the magnetic actuation set-up; J.V. and M.H. performed the magnetic

actuation experiments on marbles (J.V.) and drops (J.V., M.H.) under supervision of M.A., M.M., and D.B.; J.V. and M.A. performed the surface deformation experiments; N.K. performed the theoretical work; all authors analyzed the data; D.B. wrote the paper with contributions from all authors.

## Conflict of interest

The authors declare no conflict of interest.

**Keywords:** drops · liquid marbles · liquid transport · magnetic control · microfluidics

**How to cite:** *Angew. Chem. Int. Ed.* **2017**, *56*, 16565–16570  
*Angew. Chem.* **2017**, *129*, 16792–16797

- [1] G. M. Whitesides, *Nature* **2006**, *442*, 368–373.
- [2] R. B. Fair, *Microfluid. Nanofluid.* **2007**, *3*, 245–281.
- [3] D. Baigl, *Lab Chip* **2012**, *12*, 3637–3653.
- [4] N. J. Cira, A. Benusioglio, M. Prakash, *Nature* **2015**, *519*, 446–450.
- [5] J. B. Brzoska, F. Brochard-Wyart, F. Rondelez, *Langmuir* **1993**, *9*, 2220–2224.
- [6] O. D. Velev, B. G. Prevo, K. H. Bhatt, *Nature* **2003**, *426*, 515–516.
- [7] F. Mugele, J.-C. Baret, *J. Phys. Condens. Matter* **2005**, *17*, R705–R774.
- [8] K. Ichimura, S.-K. Oh, M. Nakagawa, *Science* **2000**, *288*, 1624–1626.
- [9] J. Berná, D. A. Leigh, M. Lubomska, S. M. Mendoza, E. M. Pérez, P. Rudolf, G. Teobaldi, F. Zerbetto, *Nat. Mater.* **2005**, *4*, 704–710.

- [10] A. Diguët, R. M. Guillermic, N. Magome, A. Saint-Jalmes, Y. Chen, K. Yoshikawa, D. Baigl, *Angew. Chem. Int. Ed.* **2009**, *48*, 9281–9284; *Angew. Chem.* **2009**, *121*, 9445–9448.
- [11] A. Diguët, H. Li, N. Queyriaux, Y. Chen, D. Baigl, *Lab Chip* **2011**, *11*, 2666–2669.
- [12] A. Venancio-Marques, F. Barbaud, D. Baigl, *J. Am. Chem. Soc.* **2013**, *135*, 3218–3223.
- [13] A. Venancio-Marques, D. Baigl, *Langmuir* **2014**, *30*, 4207–4212.
- [14] N. T. Nguyen, *Microfluid. Nanofluid.* **2012**, *12*, 1–16.
- [15] N. Pamme, *Lab Chip* **2006**, *6*, 24–38.
- [16] J. M. D. Coey, R. Aogaki, F. Byrne, P. Stamenov, *Proc. Natl. Acad. Sci. USA* **2009**, *106*, 8811–8817.
- [17] P. Brown, A. Bushmelev, C. P. Butts, J. Cheng, J. Eastoe, I. Grillo, R. K. Heenan, A. M. Schmidt, *Angew. Chem. Int. Ed.* **2012**, *51*, 2414–2416; *Angew. Chem.* **2012**, *124*, 2464–2466.
- [18] E. Bormashenko, R. Pogreb, Y. Bormashenko, A. Musin, T. Stein, *Langmuir* **2008**, *24*, 12119–12122.
- [19] N.-T. Nguyen, G. Zhu, Y.-C. Chua, V.-N. Phan, S.-H. Tan, *Langmuir* **2010**, *26*, 12553–12559.
- [20] J. V. I. Timonen, M. Latikka, L. Leibler, R. H. A. Ras, O. Ikkala, *Science* **2013**, *341*, 253–257.
- [21] Z. Long, A. M. Shetty, M. J. Solomon, R. G. Larson, *Lab Chip* **2009**, *9*, 1567.
- [22] C. H. Ooi, N.-T. Nguyen, *Microfluid. Nanofluid.* **2015**, *19*, 483–495.
- [23] J. R. Dorvee, A. M. Derfus, S. N. Bhatia, M. J. Sailor, *Nat. Mater.* **2004**, *3*, 896–899.
- [24] Y. Zhao, Z. Xu, M. Parhizkar, J. Fang, X. Wang, T. Lin, *Microfluid. Nanofluid.* **2012**, *13*, 555–564.
- [25] M. K. Khaw, C. H. Ooi, F. Mohd-Yasin, R. Vadivelu, J. S. John, N.-T. Nguyen, *Lab Chip* **2016**, *16*, 2211–2218.
- [26] P. Aussillous, D. Quéré, *Nature* **2001**, *411*, 924–927.
- [27] N. Kavokine, M. Anyfantakis, M. Morel, S. Rudiuk, T. Bickel, D. Baigl, *Angew. Chem. Int. Ed.* **2016**, *55*, 11183–11187; *Angew. Chem.* **2016**, *128*, 11349–11353.
- [28] C. R. Reisin, S. G. Lipson, *Appl. Opt.* **1996**, *35*, 1120.
- [29] P. Laird, N. Caron, M. Rioux, E. F. Borra, A. Ritcey, *Appl. Opt.* **2006**, *45*, 3495.
- [30] C. H. Ooi, A. Van Nguyen, G. M. Evans, D. V. Dao, N.-T. Nguyen, *Sci. Rep.* **2016**, *6*, 38346.
- [31] C. H. Ooi, R. K. Vadivelu, J. St John, D. V. Dao, N.-T. Nguyen, *Soft Matter* **2015**, *11*, 4576–4583.
- [32] G. McHale, M. I. Newton, *Soft Matter* **2015**, *11*, 2530–2546.
- [33] G. M. Whitesides, B. Grzybowski, *Science* **2002**, *295*, 2418–2421.
- [34] D. L. Hu, J. W. M. Bush, *Nature* **2005**, *437*, 733–736.
- [35] A. W. Martinez, S. T. Phillips, M. J. Butte, G. M. Whitesides, *Angew. Chem. Int. Ed.* **2007**, *46*, 1318–1320; *Angew. Chem.* **2007**, *119*, 1340–1342.
- [36] M. S. Bhamla, B. Benson, C. Chai, G. Katsikis, A. Johri, M. Prakash, *Nat. Biomed. Eng.* **2017**, *1*, 9.

Manuscript received: October 16, 2017

Revised manuscript received: November 3, 2017

Accepted manuscript online: November 12, 2017

Version of record online: November 12, 2017